

Integrating Geological Uncertainty into Geothermal Reservoir Simulations with Bayesian Optimization Workflows

Jeremy Rihet¹, Mohammed Abd-allah¹, Sophie Pearson-Grant² and James Patterson³

¹ AspenTech, 56A Coonan Street, Indooroopilly, Queensland, Australia

² GNS Science, Wellington, New Zealand

³ ETH Zurich, Zurich, Switzerland

*jeremy.rihet@aspentech.com

Keywords: *Modelling framework, Geothermal Reservoir Simulation, Waiwera, Automation, Aspen SKUA, Aspen Tempest ENABLE.*

ABSTRACT

Geothermal reservoir predictions are typically done under a high degree of uncertainty. Hence, accurately understanding and factoring in all uncertainties is critical for robust resource development and management. This study presents an integrated workflow that combines geological uncertainty quantification, Bayesian optimization, and automated history matching for geothermal reservoir simulation. Using a fully controlled modelling environment, with SKUA for geomodelling and Waiwera for simulation, we construct a synthetic geothermal reservoir exhibiting features typical of New Zealand such as a clay cap and heterogeneous lithologies. In addition to flow-governing reservoir uncertainties such as rock permeability and upflow rate, we account for spatial uncertainty in geologic features such as clay cap depth, clay cap hole size, permeable reservoir extent, and fault dip/strike/extent, which are progressively constrained through Bayesian Optimization techniques. The approach leverages a workflow orchestrator to automate the Natural State Calibration and the dynamic History Matching phases. Multiple realizations of the reservoir model are generated and compared against synthetic production data. To address the high computational cost of ensemble methods, we use established assisted history matching tools that support uncertainty sampling, ensemble management, calibration point setup, and efficient matching with several optimization algorithms available. The result is an ensemble of calibrated, geologically consistent reservoir models with quantified predictive uncertainty. This work demonstrates a proof of concept for a systematic and practical approach for geothermal reservoir forecasting. Because the workflow is built around a modular, software-agnostic orchestrator, a wide number of setups using different modelling approaches can be efficiently integrated within the larger history-matching framework. This flexibility offers a scalable path for researchers and operators wanting to integrate the impact of geological uncertainty into their reservoir predictions.

1. INTRODUCTION

Numerical reservoir modelling is essential to the development and sustainable management of geothermal systems. These models enable forecasting of fluid flow, heat transport, and steam production over time, which are crucial for optimizing long-term field performance. While the TOUGH family of codes have been the industry standard for the last decades, the next generation of geothermal reservoir simulators have become increasingly common, with improved coupling of

physical processes (Franz & Clearwater 2021) and parallelization to speed up simulations (Croucher et al. 2020).

Despite these improvements, uncertainty in subsurface characterization remains a fundamental limitation in reservoir modelling. Even with advanced geophysical techniques and processing, such as magnetotellurics (Bertrand et al. 2012) and gravity modelling (Stagpoole et al. 2021), estimating key reservoir properties (e.g. permeability, porosity, fracture distributions) remains challenging. Although these indirect and non-unique data can be tied to existing wells for more robust interpretations, data between and outside of wells remains highly uncertain.

Ensemble-based reservoir modelling has been used to address these issues (Dekkers et al. 2022). By generating multiple realizations of a reservoir model and perturbing rock parameters, operators can simultaneously investigate a range of possible system behaviors and quantify uncertainty. However, techniques currently used for geothermal model inversion or forecasting inherently assume a fixed geological model, which may introduce bias if the true subsurface structures do not align with the model. Several modelling techniques have been developed to address geological uncertainty in reservoir models. Multiple-point geostatistics and rules-based modelling are widely used in hydrocarbon reservoir settings, where dense well data and high-resolution geophysical data enable detailed conditioning. However, these methods are less effective in systems with sparse data and complex structures, faulting, deformation typical of New Zealand geothermal reservoirs. In such settings, stochastic geological modeling offers a more flexible approach, generating ensembles of geological realizations by sampling from defined statistical distributions that represent uncertainty in structure features and lithological boundaries (de Beer et al 2025). This allows modelers to account for key geological unknowns (e.g. fault extent, location, and permeable zone connectivity) in a probabilistic framework that supports risk-based decision making.

This study applies these ideas to geothermal systems by performing assisted history matching to an ensemble of simulations with varying geological parameters and rock properties. We use SKUA to generate multiple geological model realizations of a synthetic reservoir typical of New Zealand, then use Waiwera to simulate the natural state and production history of the model. A single sample from the prior parameter distribution is taken as a ground truth and synthetic observations of wellbore temperature profile and feed point pressure and enthalpy are created. The model is then calibrated using iterative Bayesian Optimization techniques to create progressively narrower posterior distributions until the ensemble has converged on the ground truth case observations.

2. METHODOLOGY

2.1 Geological Model Creation

Developing a robust static geological model for geothermal simulation requires synthesizing information from multiple data sources and disciplines. The model serves as a framework to represent the key subsurface features affecting the fluid flow—defining the upflow zones, the recharge regions, the reservoir extent, and the different geological features such as the faults or the volcanic alteration zones.

In practice, this is typically achieved in three steps by using commercial geomodelling tools available in the market. First, a conceptual model is created by integrating and interpreting the various geothermal data types – from geophysical or well measurements to geological concepts. This is then converted into a 3D mesh populated with thermodynamic properties and rock properties. Finally, this grid is exported to a geothermal simulator in a dedicated format, where boundary and production/injection terms are included.

For this study, we leveraged Aspen SKUA's advanced modeling capabilities to construct a synthetic geothermal reservoir model. The model illustrated in Figure 1 incorporates key geothermal features, including a permeable reservoir, an overlying clay cap, bounding impermeable zones, and fault structures. A structural model incorporating the horizons and fault surfaces was first constructed, with each geological feature defined using surface-based modelling tools. These surfaces were then upscaled and transferred onto a rectilinear grid as discrete grid regions. Circular-shaped features such as the clay hole, impermeable boundaries, and upflow zones were initially defined as curve objects and similarly mapped to grid regions. The various grid regions were subsequently combined according to geological rules to generate the final geocellular model.

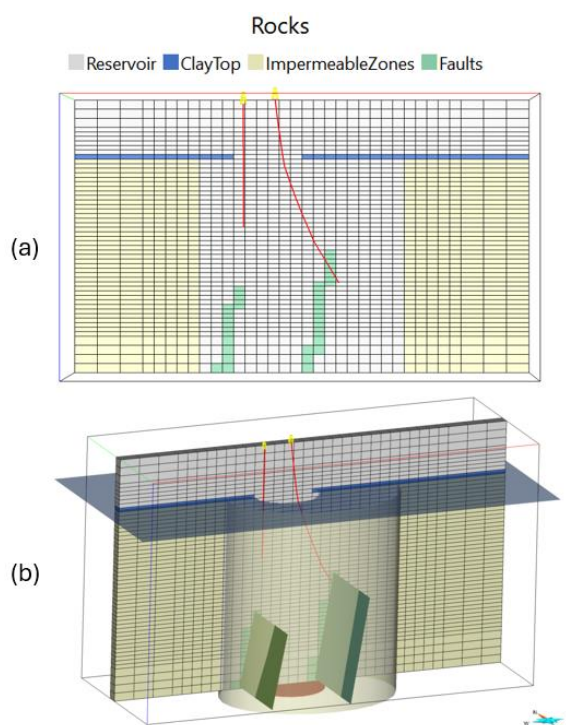


Figure 1: (a) 2D Slice of the Synthetic Model (b) Position of the Rock Boundaries and of the upflow zone in 3D

2.2 Geological Uncertainties Parametrization

Because of a general lack of data reliability away from the wells, geothermal models often have a high degree of geological uncertainty associated with them. It is essential to account for this uncertainty when using these models for predicting the subsurface behavior.

To reflect this uncertainty, multiple realizations of the static model must be generated. Each scenario captures a different but geologically plausible configuration of the reservoir. To support the generation of these multiple scenarios, the modelling software used must offer full traceability for the model construction and must allow it to be automatically rerun using different values for the parameters it used during this process. Since many parameters are involved, it is a usual practice to identify the parameters we consider relevant for our model and flag them as variable.

In our example, we have defined as variable the uncertainties for the clay cap depth, for the clay hole size and position, for the faults extent and position, for the reservoir extension and for the size of the upflow zone. Figure 2 shows examples of different realizations generated automatically from the parametrized geological uncertainty. Some parameters, such as clay cap depth, are estimated from geophysical data but may contain some uncertainty; other parameters are difficult to estimate, such as the extent of a fault below existing wells or the lateral extent of the permeable reservoir.

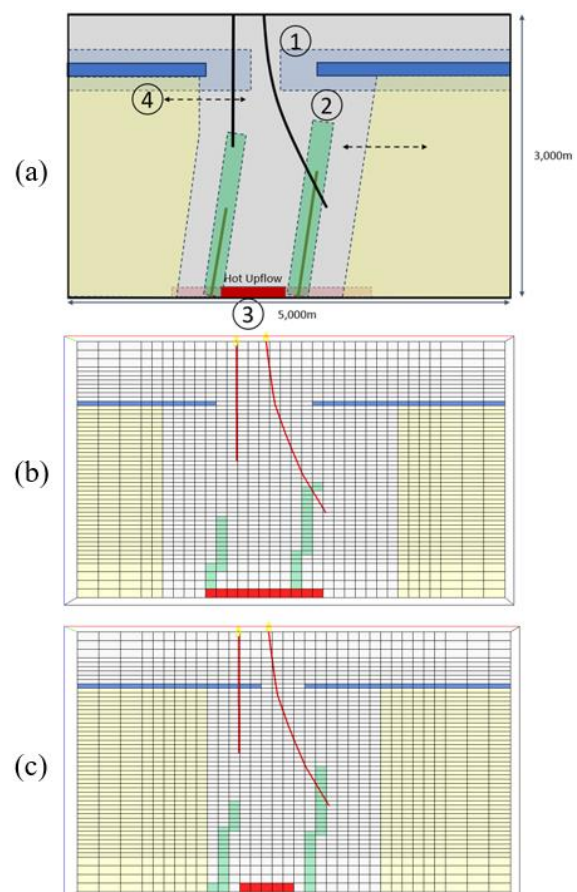


Figure 2: (a) Sketch Representation of the Geological Uncertainties (b) Geological Realization with a large clay hole, a large reservoir extent and a large upflow zone (c) Geological Realization with a small offset clay hole, a small reservoir extent and a small upflow zone

2.3 Waiwera Project Set Up and Simulation

Once the suite of geological models has been generated in SKUA, each realization can be exported for simulation using the export macro developed by Rihet (2023). This step translates the generated static models into ready-to-run simulation decks, without an additional manual data preparation step. Recent enhancements to the macro include automatic configuration of Neumann boundary conditions using prescribed heat fluxes, as well as support for batch definition of complex model components. Numerous rock types and source terms—often required in geothermal simulations—can now be defined through structured tables. These improvements were made to ensure scalability for large ensemble-based workflows essential for uncertainty quantification.

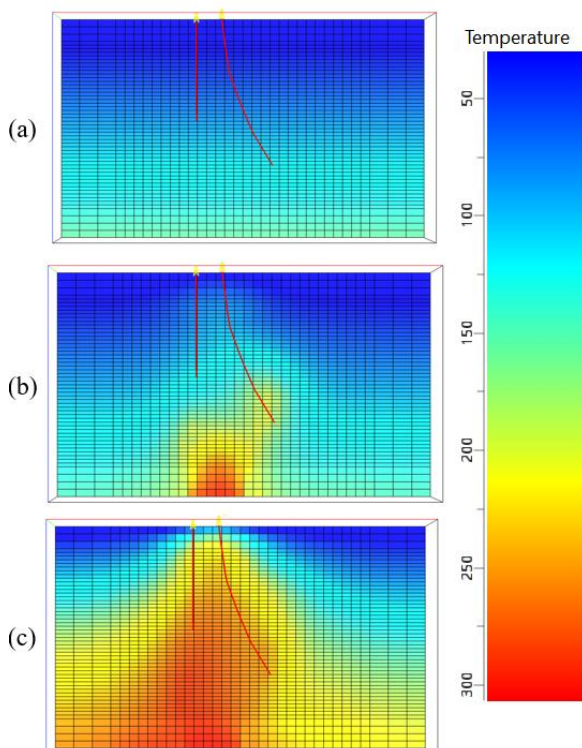


Figure 3: Temperature Evolution for the Natural State Model Simulation at (a) $t = 0$ (b) $t = 3000$ years (c) $t = 30000$ years

In our example, we have run all our scenarios through a Natural State Simulation, followed by a Historical Simulation where wells were added as sources. Figure 3 shows the Natural State simulation results for one of the geological realizations. The full parameter table is given in Figure 6.

2.4 Integration within a Workflow Orchestrator

As demonstrated by Rihet (2023), both the preprocessing phase—model export and input deck preparation—and the simulation phase in Waiwera are fully scriptable. This makes them ideal candidates for integration into a workflow orchestrator such as Aspen Tempest Enable. The underlying principle is straightforward: each software component is treated as a command-line executable, with all relevant parameters passed as arguments. These parameters can be programmatically adjusted by the orchestrator between runs. Since all jobs are monitored through a run tracking interface, in case a simulation fails to converge or encounters early termination, the runs are flagged and the collected log outputs can be used for issue diagnosis. The user may choose to rerun the simulation later if deemed necessary.

As illustrated in Figure 4, the workflow can be flexibly customized to match the modeling objective. For example, a Natural State Model simulation workflow may only involve exporting a geological model from SKUA, running the simulation, and comparing the output against a calibration end point. If a Historical Simulation is desired, an additional step can be inserted where well sources are introduced in a second simulation run. batch mode operations are defined in an XML file, including which SKUA commands are called, whether the HDF5 results are extracted and loaded in Enable, or whether a Python script is executed to prepare a JSON file for the historical simulation.

Chaining modular components this way allows the orchestrator to automatically execute a predefined workflow with different values for the parameters set as variables. The complexity of the workflows executed within each component relies on the level of automation permitted by the software. In this case, the automatic re-generation of a structural model is made possible by the geomodelling software ability to record and execute at once all steps of the modelling workflow.

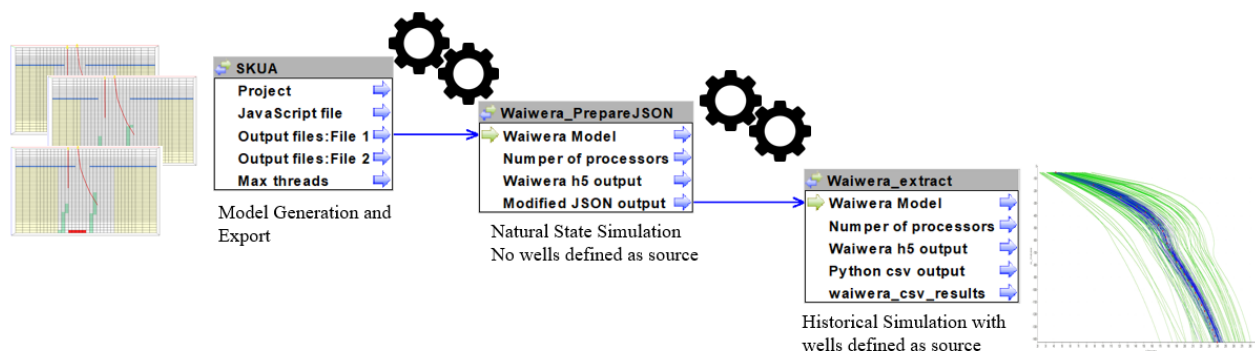


Figure 4: Integration example of SKUA and Waiwera as different “workflow components” within Tempest ENABLE.

2.5 Uncertainty optimization with Assisted History-Matching Algorithms

Once the different workflow components have been correctly configured, the workflow orchestrator will be able to manipulate the parameters flagged as variables and evaluate their influence on the simulation outcomes. This enables the setup of assisted history matching workflows, where the software iterates on the parameter values to minimize the simulation response misfit with the historical data.

The process begins with a **scoping phase** during which the goal is to assess whether the prior parameter distribution results in geological realizations that bracket the observed data. Different techniques such as Latin Hypercube Sampling (LHS) or maximin design are available to sample the uncertainty space. If the initial ensemble fails to contain the historical trends, the initial uncertainty ranges will need to be revisited.

In practice, uncertainty optimization requires **defining estimator points**—key measurements to be matched—and assigning a tolerance range around them. These points will then serve as targets for the optimization algorithm. The estimator points can be set simultaneously on various properties like the measured pressure, temperature, ground surface deformation, or even set economics goals – to name a few. As shown on Figure 5, they can be set on each grid cell across multiple time steps – to match the dynamic properties – and on the well profile at given time steps, in which case the model will aim to match the general vertical property trend.

The next step is to **select an appropriate assisted history-matching (AHM) algorithm**. Different methods are available:

- **Proxy-based approaches**, which use surrogate models to approximate simulator responses and reduce computational cost [Fillacier et al., 2014]
- **Ensemble-based methods**, such as the Ensemble Smoother with Multiple Data Assimilation [Abdallah et al., 2021]

As outlined in Section 2.4, the AHM algorithm can be configured to target the Natural State Model, the Historical Simulation, or both. For example, models can be initially constrained by Natural State calibration to reduce the ensemble, and then further refined via historical matching. It is also possible to integrate the Natural State model simulation but only constrain the ensemble using the historical production data if this initial uncertainty reduction step is not necessary.

In our case, since this study uses a synthetic dataset, we defined a “ground truth” parameter set a priori and generated synthetic observations accordingly. The initial uncertainty range for the geological parameters is shown in Figure 6. Because a vapor phase would appear in some cases, significantly slowing down the simulations, these ranges were initially constrained with a Natural State Model Calibration with a Proxy-based approach using a fully liquid model as a target. Estimator points were set simultaneously on the dynamic trends and the spatial trends for the well pressures and temperatures. These constrained ensembles were then refined further in a second step using an Ensemble-based method on the historical production data (cf. Figure 5).

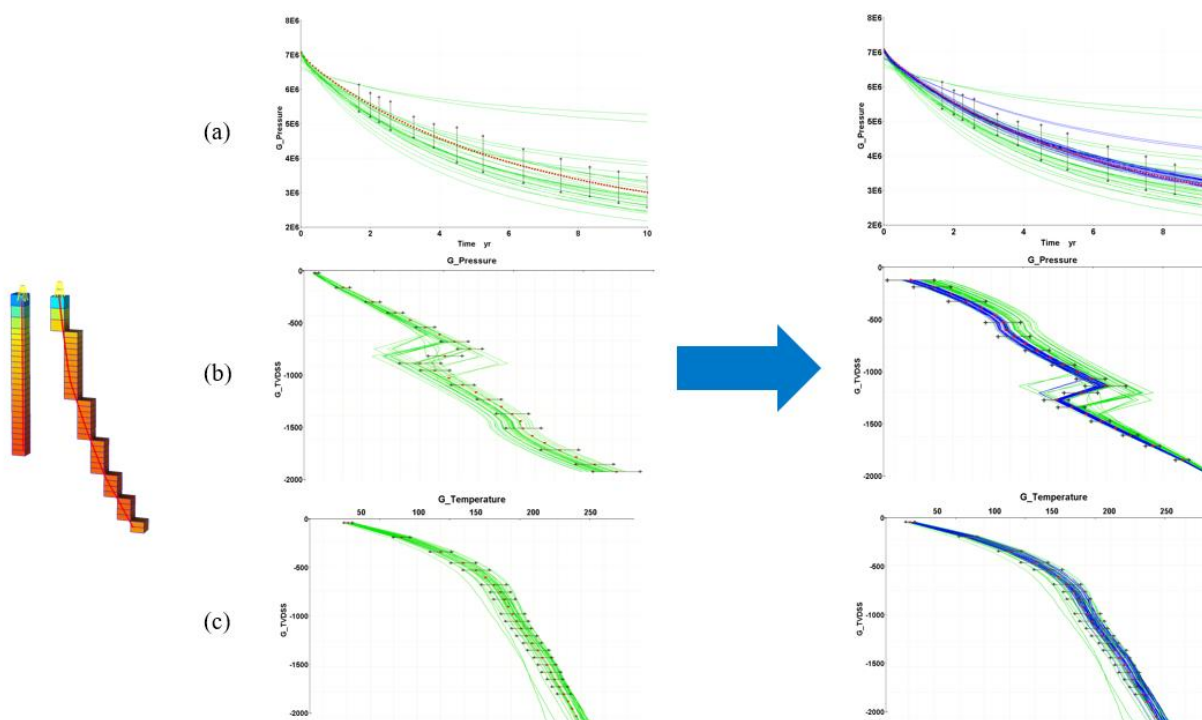


Figure 5: Ensemble-based History Matching Results with Prior (Green) and Posterior (Blue) Ensembles for the (a) Bottom well Pressure over 10 years (b) Vertical Well Pressure profile at t=10 years (c) Vertical Well Temperature Profile at t=10 years

Name	Active	Correlated	Min	Max	Most Likely	Focus Min	Focus Max	Distribution	Transform	Type	Sample
ClayHole_Radius	<input checked="" type="checkbox"/>	<input type="checkbox"/>	200.0	600.0	400.0			Gauss	Linear	Geology	Continuous
ClayTopShift	<input checked="" type="checkbox"/>	<input type="checkbox"/>	-100.0	100.0	0.0			Triangle	Linear	Geology	Continuous
Fault1_Extension	<input checked="" type="checkbox"/>	<input type="checkbox"/>	0.0	100.0	0.0			PERT	Linear	Geology	Continuous
Fault1_Shift	<input checked="" type="checkbox"/>	<input type="checkbox"/>	-50.0	50.0	0.0			Uniform	Linear	Geology	Continuous
Fault2_Extension	<input checked="" type="checkbox"/>	<input type="checkbox"/>	0.0	100.0	0.0			PERT	Linear	Geology	Continuous
Fault2_Shift	<input checked="" type="checkbox"/>	<input type="checkbox"/>	-50.0	50.0	0.0			Uniform	Linear	Geology	Continuous
Impermeable_MajorRa...	<input checked="" type="checkbox"/>	<input type="checkbox"/>	1000.0	1400.0	1100.0			Gauss	Linear	Geology	Continuous
Impermeable_MinusRa...	<input checked="" type="checkbox"/>	<input type="checkbox"/>	500.0	900.0	800.0			Gauss	Linear	Geology	Continuous
Porosity_Reservoir	<input checked="" type="checkbox"/>	<input type="checkbox"/>	0.05	0.1	0.1			Triangle	Sqrt	Geology	Continuous
Radius_Upflow_Zone	<input checked="" type="checkbox"/>	<input type="checkbox"/>	250.0	750.0	500.0			Gauss	Linear	Geology	Continuous
Upflow_Rate	<input checked="" type="checkbox"/>	<input type="checkbox"/>	5.0	20.0	5.0			Triangle	Sqrt	Geology	Continuous
XCenter_Clay_Hole	<input checked="" type="checkbox"/>	<input type="checkbox"/>	2938.0	3338.0	3138.0			Gauss	Linear	Geology	Continuous
XCenter_Impermeable...	<input checked="" type="checkbox"/>	<input type="checkbox"/>	3300.0	3700.0	3500.0			Uniform	Linear	Geology	Continuous
YCenter_Clay_Hole	<input checked="" type="checkbox"/>	<input type="checkbox"/>	3800.0	4200.0	4000.0			Gauss	Linear	Geology	Continuous

Figure 6: Parameter Initial Uncertainty Ranges and Sampling Modes

2.6 Post-Processing and Analysis

After the assisted history matching phase, the resulting model set must be thoroughly analyzed to better understand what was done during the optimization process and what it means for the future predictions the model ensembles can provide. This is facilitated by the AHM post-processing and analysis tools available in Aspen Tempest Enable.

The first and most straightforward result to examine is how the parameter ranges have shifted during history matching. This is usually done by comparing prior and posterior distributions of the uncertain parameters. After this, it is often necessary to analyze joint parameter behavior to understand whether parameters exhibit compensatory effects or non-linear interdependencies. Visualization tools like scatter plots, parallel coordinates plots and correlation maps are valuable for detecting patterns that may not be evident when inspecting parameters in isolation.

To complement this, sensitivity analysis can be performed on the calibrated ensemble. Tornado plots or variance-based rankings help quantify which parameters have the largest

impact on objective function outcomes or on production forecasts. Quality views also help to check the evolution of the history match quality over the runs.

These post-processing tools are critical to transform the ensemble from a black box of model outputs into an informed result that can be used for the evaluation of field development plans.

Figure 7 shows an example of a dashboard built from the natural state model calibration process. Data science tools help to build customized plots looking at the parameter's impact on the simulation results. Interactive cross-filtering options (where the plots can dynamically interact with each others) are also important tools for engineers to efficiently analyze and process the results.

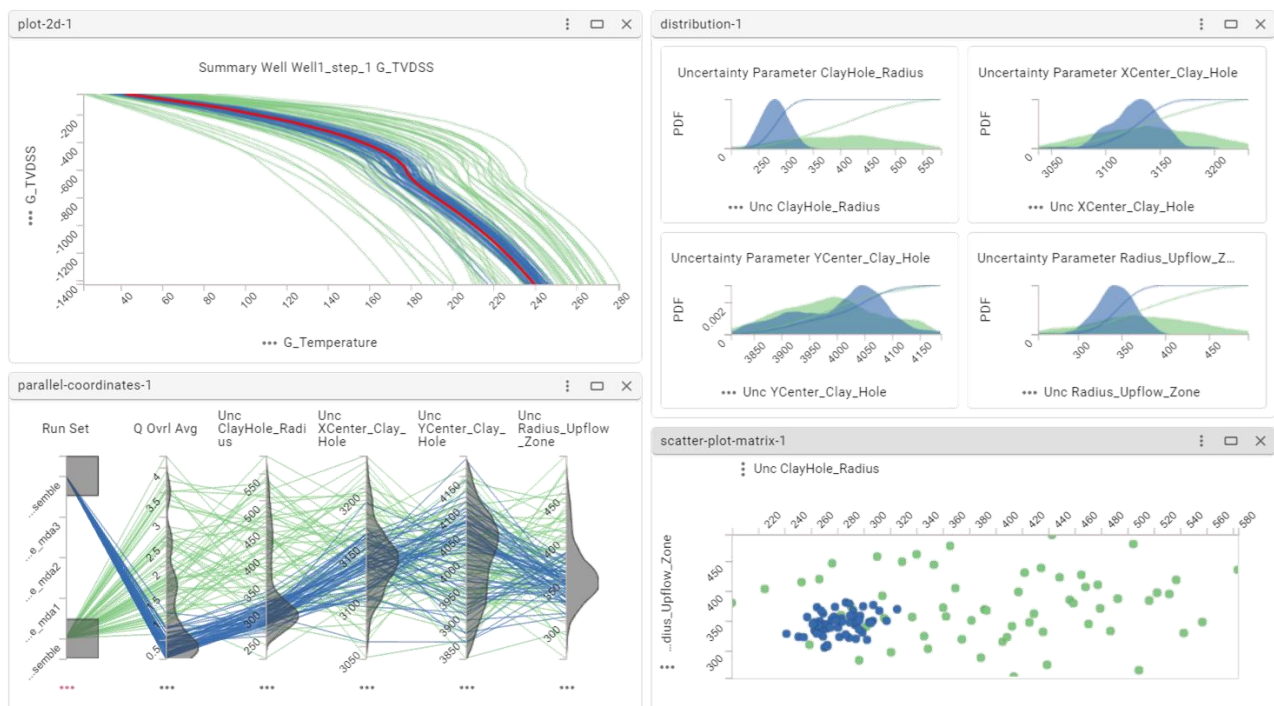


Figure 7: Analytics Dashboard Comparing Prior (Green) and Posterior (Blue) Ensembles using Standard Uncertainty Analysis Plots. The multi-dimension parallel coordinate plot shown in the lower left helps quickly comparing the parameter value spread for the different ensembles, highlighting possible correlations between the variables.

3. RESULTS

3.1 Simulation-Driven Uncertainty updates

The uncertain parameters defined as variables for the synthetic case exhibited different sensitivity to the optimization processes.

Some parameters, such as the size of the upflow zone or the upflow rate, exhibited high sensitivity during the Natural State calibration phase—meaning they had a strong influence on the objective function—and their value ranges were consequently narrowed in the subsequent history matching step. Other parameters like the position of the clay top showed low sensitivity to the calibration process but higher sensitivity to the history match process. This could be explained by the fact that the pressure profiles of the natural state models were fairly similar, but once production commenced, the clay cap depth had a stronger influence on the pressure changes.

Last, some parameters like the extent of the impermeable zone seemed relatively insensitive to the optimization processes when just considering the posterior distribution. However, it is worth noting that these parameters could exhibit interdependencies with other parameters that the raw histogram could fail to capture, and that they could also still be of importance for the prediction phase.

In addition to the dashboard view presented in the previous section, if the parameters are related to the structural geology in nature, they can be created as formation boundary objects and visualized in 3D, as presented in Figure 9. To create this view, the parameter values used to generate the ensemble runs were exported as a table and read by the modelling platform. Then, the ensembles were color-coded as the following: Red for the initial scoping runs, blue for the natural state calibrated runs, green for the history-matched runs, and black for the “ground truth” realization.

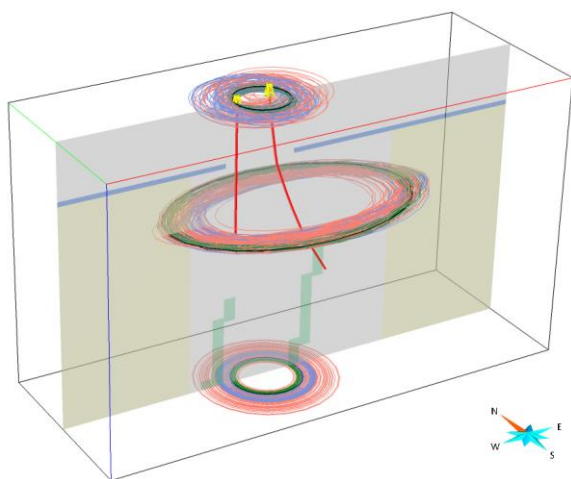


Figure 9: Realizations for the Clay Hole Position (Top Curves), Reservoir Extent (Middle Curves) and Upflow Zone (Bottom Curves).

Last, some parameters' uncertainty range was not sufficiently large to have a significant effect on the model. For example, the faults position were set within a 100m uncertainty envelope, which is not very significant when compared to the areal cell resolution. Similarly, the fault extension PERT sampling mode has had the tendency to skew the faults definition towards their base-case.

3.2 Combined Static and Dynamic Impact Assessment

One of the major benefits of the approach presented in this paper is the simultaneous inclusion of structural parameters (such as the clay cap configuration or the fault's position), flow-related parameters (such as the features porosity or the upflow rate) and reservoir engineering parameters (such as the well locations or production rates). How those parameters are concomitantly updated can be analyzed to fully understand the model behavior. In real case-studies, specific parameter combinations may produce results that are considered more or less likely by the convergence algorithms, allowing engineers to assess the probability of specific scenarios as far as historical production data are concerned.

One good illustration of this situation is the formation or the absence of a gas cap during the scoping phase. Rather than happening because of a single parameter value, an analysis revealed that the core reason was the alignment of the clay hole and the upflow zone. Broadly speaking, if the clay hole was relatively misaligned with the upflow zone and the upflow rate was consequent, gas would be created above the clay cap during simulation. Conversely, if the clay hole was well aligned and would allow passage of the fluid moving in an upward direction, steam would not form during simulation even with high upflow rates (cf. Figure 10).

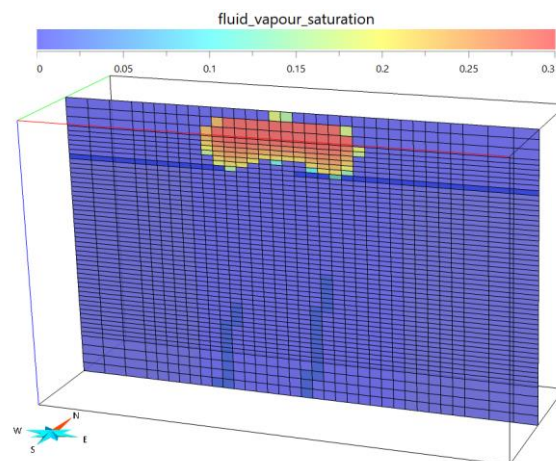


Figure 10: Gas Saturation property shown on a realization with a Gas Cap

In this case, the presence or the absence of a gas cap is directly related to the ambient pressure and temperature conditions – variables that were defined as estimator points. Because of this, it is straightforward for the optimization process to converge towards one dominant scenario. In more ambiguous cases, where multiple scenarios are plausible from a history-matching standpoint, the relative frequency of realizations falling into each category can provide a measure of their likelihood.

3.3 Evergreen modelling approach

One of the key advantages of this scripted, modular setup is its ability to support evergreen modelling. Because the geological model is built from parameterized and repeatable steps, incorporating new data—such as updated geophysics, production history, or well data—can be done with minimal manual intervention by using the predefined processes. This helps to significantly shorten the model update cycle when new data comes in.

3.4 Probabilistic Production Predictions

One of the most powerful advantages of ensemble-based workflows is the ability to generate probabilistic forecasts that explicitly account for subsurface uncertainty. Rather than relying on a single deterministic model, predictions are made across an ensemble of calibrated realizations, each honoring both geological plausibility and historical data. This provides a distribution of possible outcomes for any forecasted scenario—critical for decision-making under uncertainty (Bordas et al. 2020).

To illustrate this, we conducted two test predictions involving the forecasting of a planned production well using the parameters posterior ensembles. In the first scenario, the well was placed in a part of the reservoir identified with high confidence across all realizations as permeable. In the second scenario, the well was positioned in a region where the well would be in the reservoir zone in some realization, and in the impermeable zone in others.

The results shown in Figure 11 highlight the main benefits of the approach: in the first case, the planned well performance can be estimated probabilistically, and in the second case, the impact of a given geological uncertainty on the production forecasts can be fully apprehended. The latter result shows that even when certain parameters—like the precise extent of the impermeable zone—are not strongly constrained during history matching, their uncertainty can still significantly affect forecast outcomes. Such behavior underscores the need to preserve geological variability throughout the workflow, especially when using the ensemble for risk mitigation or economic evaluation.

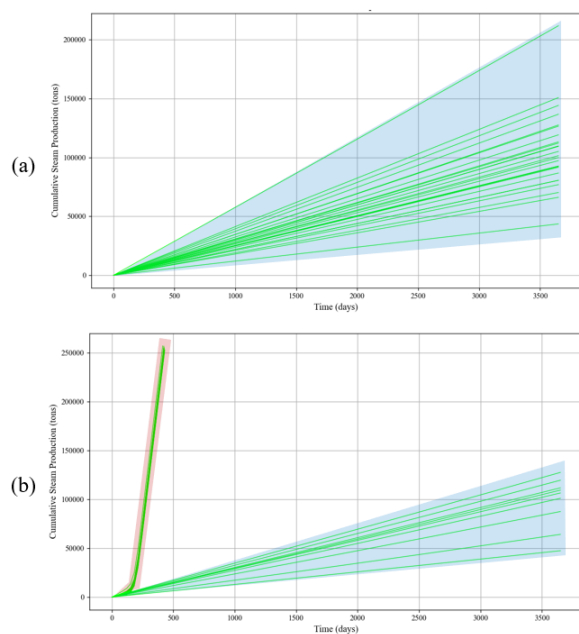


Figure 11: 10-year cumulative steam production forecast envelopes for a planned well located in (a) a consistently permeable zone and (b) a region of high geological uncertainty. Realizations located in the red envelope showing high steam production are the realizations for the well located in the impermeable zone.

3.5 Stochasticity Integration

Another important aspect of the assisted history matching framework is its compatibility with the stochastic modelling algorithms available in many geomodelling software to generate multiple structural realizations or multiple rock property scenarios. Even if stochasticity cannot be used as a control variable during history matching, it serves as a valuable means to characterize internal variability and assess forecast robustness. In the calibration phase, this stochastic noise is treated as background variability—preserved for interpretation but not targeted for minimization.

4. DISCUSSION

While the proposed workflow offers a robust framework for integrating geological uncertainty into geothermal forecasting, the implementation details within each component can vary significantly depending on the software ecosystem and depending on the modelling approach. In principle, the workflow is highly customizable, and users can tailor workflow steps to suit project-specific needs. These customizable steps include simulation preprocessing, simulation, post-processing, and optimization processes. However, this flexibility is inherently bound by how adaptable the underlying tools are to automation and external control.

In our case, this included developing the export macros in Aspen SKUA to expose parameter variables, as well as developing Python scripts to manage simulation inputs, extract HDF5 outputs, and inject source terms for historical scenarios. While this customization enables a tight integration of the various workflow components, creating the input macro in Aspen SKUA does require proficiency with the tool. Currently, some of the logic remains embedded in hard-coded routines, suggesting a potential area for future improvement in user interface design once typical geomodelling workflows and simulation set up have been identified, with the objective to make such approaches more broadly accessible across the geothermal modelling community.

Although the model used in this study is synthetic and deliberately simplified, the workflow still provided valuable insights with potential relevance to real-world applications. The goal of this exercise was to test and demonstrate the workflow's ability to reveal relationships between uncertain parameters and model responses: In doing so, the software highlighted subtle but meaningful dynamics that would likely manifest in more complex settings. For instance, in the Natural State calibration phase, many model realizations tended toward pressure equilibrium by the end of the simulation. As a result, pressure alone offered limited discriminatory power between realizations, and temperature profiles emerged as a more informative matching target during this stage. However, for the Historical Simulation phase, the onset of production caused pressure to diverge more significantly across runs. This made pressure drawdown patterns a more sensitive indicator of reservoir behavior, shifting the importance toward parameters that govern dynamic response. These evolving sensitivities impacted how parameters were ranked and updated throughout the workflow. During Natural State calibration, the most influential parameters were those controlling phase behavior, such as clay cap geometry and the size and intensity of the upflow zone, while during the history matching phase, parameters such as porosity and the radius of the impermeable zone gained more prominence.

With the relatively small number of parameters taken as variable in this synthetic example, a proxy-based modelling approach proved to be the most effective history-matching method. In real case-studies with thousands of modifiers, the ensemble smoother method would be preferred, but combining the two methods also remains a possible option. In this paper, a multi-stage optimization process was done so cases with a gas cap could be quickly discarded, revealing as a result layered sensitivities. In a real-case scenario, a similar initial uncertainty reduction step could be applied to the geological uncertainty parameters that we anticipate to have the biggest impact on the production forecast for the field studied, effectively acting as an initial filtering step (Powers et al. 2023).

Ultimately, choosing which history-matching approach is best depends on the data available, our understanding of the uncertainties at play and what the analysis of the optimization process reveals when trying to match historical data.

5. CONCLUSION

This study presents a fully integrated workflow using established commercial tools for incorporating geological uncertainty into geothermal reservoir forecasting. By leveraging the advanced modelling capabilities of Aspen SKUA, the simulation power of Waiwera, and the automation features of Tempest Enable, we demonstrate a flexible and scalable approach for generating geologically consistent ensembles and calibrating them against historical or synthetic data. This workflow addresses several common pain points in geothermal modelling: it facilitates automation of complex model-building tasks, supports the design of structured optimization processes, and enables efficient analysis of ensemble results to build a deeper understanding of system behavior. This offers several practical applications such as the prediction of planned well performances, making use of both the evergreen nature of the modelling process and the probabilistic forecasting capabilities of ensemble methods.

That said, fully automating the modelling process is still non-trivial. Current implementations require significant customization and scripting, particularly during the geomodelling and input preparation stages. Looking ahead, the next logical step would be to apply this workflow to a real geothermal field—both to validate the methodology and to help streamline geological uncertainty modelling in practical geothermal contexts.

REFERENCES

Abd-Allah, Mohammed, Abdelrahman, Ahmed, Van Den Brul, Luke, Taha, Taha, and Mohammad Ali Javed. "Probabilistic Economical Evaluation for Business Decisions Through Integrated Uncertainty Assessment and Reliable Ensemble-Based Production Forecasts." *Abu Dhabi International Petroleum Exhibition & Conference*, Abu Dhabi, UAE, Nov 2021.

de Beer, A., Bjarkason, E. K., Gravatt, M., Nicholson, R., O'Sullivan, J. P., O'Sullivan, M. J., & Maclaren, O. J. (2025). Ensemble Kalman inversion for geothermal reservoir modelling. *Geophysical Journal International*, 241(1), 580–605. <https://doi.org/10.1093/gji/ggaf060>

Bertrand, E. A., Caldwell, T. G., Hill, G. J., Wallin, E. L., Bennie, S. L., Cozens, N., Onacha, S. A., Ryan, G. A.,

Walter, C., Zaino, A., Wameyo, P. (2012) "Magnetotelluric imaging of upper-crustal convection plumes beneath the Taupo Volcanic Zone, New Zealand." *Geophysical Research Letters*, 10.1029/2011GL050177

Bordas, R. & Heritage, J.R. & Javed, Mohammad Ali & Peacock, Gavin & Taha, T. & Ward, P. & Vernon, Ian & Hammersley, R.. (2020). A Bayesian Optimisation Workflow for Field Development Planning Under Geological Uncertainty. *ECMOR XVII 1-20*. 10.3997/2214-4609.202035121.

Croucher, A.E., Osullivan, M.J., O'Sullivan, J.P., Yeh, A., Burnell, J., Kissling, W., 2020. Waiwera: a parallel open-source geothermal flow simulator. *Computer and Geosciences 141*

Dekkers, K., Gravatt, M., Maclaren, O. J., Nicholson, R., Nugraha, R., O'Sullivan, M., Popineau, J., Riffault, J., & O'Sullivan, J. (2022). Resource Assessment: Estimating the Potential of a Geothermal Reservoir. Proceedings, 47th Workshop on Geothermal Reservoir Engineering, Stanford University, Stanford, California, February 7-9, 2022. SGP-TR-223.

Fillacier S., Fincham A. E., Hammersley R. P., Heritage J. R., Kolbikova I., Peacock G. and Soloviev V.Y., (2014). "Calculating Prediction Uncertainty using Posterior Ensembles Generated from Proxy Models"; SPE-171237-MS

Franz, Peter, Clearwater, Jonathon. "Volsung: A Comprehensive Software Package for Geothermal Reservoir Simulations." Proceedings World Geothermal Congress 2020+1, Reykjavik, Iceland, April - October 2021.

Power, A., Gravatt, M., Dekkers, K., Maclaren, O. J., Nicholson, R., O'Sullivan, J., de Beer, A., Renaud, T., O'Sullivan, M. (2023). Improved filtering for a new Resource Assessment Method, *Proc. 48th Workshop on Geothermal Reservoir Engineering Stanford University*, Stanford University, Stanford, California, February 6-8, 2023. SGP-TR-224.

Rihet, J.: An Integration Solution of Geomodelling Tools in a Geothermal Modelling Framework. *Proc. 45th New Zealand Geothermal Workshop*, Auckland, New Zealand. (2023).

Siler DL, Hinz NH, Faulds JE, Tobin B, Blake K, Tiedeman A, Sabin A, Lazaro M, Blankenship D, Kennedy M, Rhodes G, Nordquist J, Hickman S, Glen J, Williams C, Robertson-Tait A, Calvin W, Pettitt, W (2016) The Geologic Framework of the Fallon FORGE Site. *Geothermal Resources Council Transactions*, v. 40, p. 573-584.

Stagpoole, Vaughan, Miller, Craig, Caratori Tontini, Fabio, Brakenrig, Thomas, and Macdonald, Nick. "A two million-year history of rifting and caldera volcanism imprinted in new gravity anomaly compilation of the Taupō Volcanic Zone, New Zealand." *New Zealand Journal of Geology and Geophysics*, 2021, Vol. 64, Nos. 2-3, 358-371.